



A Journal of the Gesellschaft Deutscher Chemiker

Angewandte Chemie

GDCh

International Edition

www.angewandte.org

Accepted Article

Title: Multifunctional Tubular Organic Cage-Supported Ultrafine Palladium Nanoparticles for Sequential Catalysis

Authors: Nana Sun, Chiming Wang, Hailong Wang, Le Yang, Peng Jin, Wei Zhang, and Jianzhuang Jiang

This manuscript has been accepted after peer review and appears as an Accepted Article online prior to editing, proofing, and formal publication of the final Version of Record (VoR). This work is currently citable by using the Digital Object Identifier (DOI) given below. The VoR will be published online in Early View as soon as possible and may be different to this Accepted Article as a result of editing. Readers should obtain the VoR from the journal website shown below when it is published to ensure accuracy of information. The authors are responsible for the content of this Accepted Article.

To be cited as: *Angew. Chem. Int. Ed.* 10.1002/anie.201908703
Angew. Chem. 10.1002/ange.201908703

Link to VoR: <http://dx.doi.org/10.1002/anie.201908703>
<http://dx.doi.org/10.1002/ange.201908703>

Multifunctional Tubular Organic Cage-Supported Ultrafine Palladium Nanoparticles for Sequential Catalysis

Nana Sun,^[a] Chiming Wang,^[a] Hailong Wang,^{*[a]} Le Yang,^[b] Peng Jin,^[b] Wei Zhang,^{*[c]} and Jianzhuang Jiang^{*[a]}

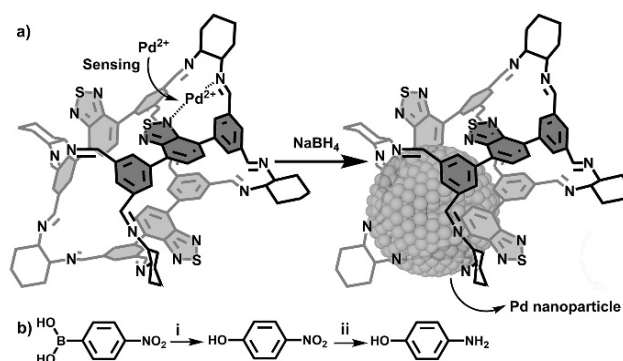
Abstract: The imine condensation reaction of 5,5'-(benzo[*c*][1,2,5]thiadiazole-4,7-diyl)diisophthalaldehyde with cyclohexanediamine resulted in a shape-persistent multifunctional tubular organic cage (MTC1). It exhibits selective fluorescence sensing towards divalent palladium ions with a very low detection limit of 38 ppb, suggesting the effective complexation between these two species. The subsequent reduction of MTC1 and palladium acetate with NaBH₄ afforded a cage-supported catalyst with well dispersed ultrafine palladium nanoparticles in a narrow size distribution of 1.9 ± 0.4 nm, denoted as Pd@MTC1-1/5. Such ultrafine palladium nanoparticles in Pd@MTC1-1/5, in cooperation with photocatalytically active MTC1, enable efficient sequential reactions involving visible light-induced aerobic hydroxylation of 4-nitrophenylboronic acid to 4-nitrophenol and the following hydride reduction with NaBH₄. The present result represents the first example of a multifunctional organic cage capable of sensing, directing nanoparticle growth, and catalyzing sequential reactions, revealing the bright perspective of this relatively new kind of porous materials.

Introduction

The rapid development of reticular chemistry initiated by metal–organic frameworks (MOFs) and covalent organic frameworks (COFs) has been witnessed in the past decades, making successive breakthroughs in the fields of gas sorption, small molecule separation, sensing, ion conduction, and heterogeneous catalysis.^[1,2] In the realm of reticular chemistry, those new porous organic frameworks including hydrogen-bonded frameworks (HOFs)^[3] and porous organic cages (POCs)^[4] constructed by the self-assembly of small molecular building blocks have attracted increasing attention due to their unique advantages in solution processing and regeneration. In particular, POCs with pre-organized molecular cavity surrounded by various heteroatoms can be regarded as one kind of special porous materials.^[4] In addition to functioning as adsorbents,^[4] the well-defined molecular cavity endows POCs as excellent hosts to selectively accommodate various guests.^[5] Ultrafine

metal nanoparticles (NPs) in the size of less than 2.0 nm can be stabilized by organic cage hosts as well, exhibiting excellent catalytic capability for various organic reactions.^[6] Thus far, utilizing the synergistic effect of ultrafine metal NPs and organic cages to facilitate organic reactions *via* two different catalytically active sites has rarely been explored, due to the lack of functionality in most cage hosts. It is therefore of significant importance to develop new functional POCs towards cage-based synergistic/sequential catalysis.^[11,5f]

In this work, a multifunctional tubular organic cage (MTC1) with both fluorescent and photocatalytic properties (Scheme 1), has been designed, synthesized, and structurally characterized by single crystal X-ray diffraction analysis. By using dynamic covalent chemistry of imine bonds,^[4] simple condensation of benzo[*c*][1,2,5]thiadiazole derivative and cyclohexanediamine afforded MTC1. Abundant nitrogen atoms decorated in the nanometer-sized cavity of MTC1 endow this POC exclusive fluorescence sensing capability towards divalent palladium ions with a very low detection limit of 38 ppb. The subsequent reduction of a solution containing MTC1 and palladium acetate with NaBH₄ afforded a catalyst, Pd@MTC1-1/5, with well dispersed ultrafine palladium nanoparticles in a narrow size distribution of 1.9 ± 0.4 nm. The ultrafine palladium NPs in Pd@MTC1-1/5, together with the photocatalytically active POC, efficiently promote two-step sequential reactions from 4-nitrophenylboronic acid *via* a 4-nitrophenol intermediate to 4-aminophenol through the visible light-induced aerobic hydroxylation followed by hydride reduction. MTC1 represents the first organic cage with multiple functionalities, opening new possibilities for exploiting the application diversity of this kind of porous matter.



Scheme 1. (a) Schematic representation of the growth of ultrafine palladium NP in the multifunctional cage MTC1 through initial binding of divalent palladium ions followed by reduction; (b) Sequential catalysis of visible light-induced aerobic hydroxylation reaction (i) and hydride reduction (ii) in the presence of Pd@MTC1 catalyst. Conditions: (i) catalyst, *i*Pr₂NEt, O₂, CD₃CN/D₂O, hv; (ii) catalyst, NaBH₄, H₂O.

[a] Dr. N. Sun, Prof. H. Wang, Dr. C. Wang, Prof. J. Jiang
Beijing Key Laboratory for Science and Application of Functional Molecular and Crystalline Materials, Department of Chemistry, University of Science and Technology Beijing, Beijing 100083, China
E-mail: hlwang@ustb.edu.cn (H.W.) and jianzhuang@ustb.edu.cn (J.J.)

[b] M.S. L. Yang, Prof. P. Jin
School of Materials Science and Engineering, Hebei University of Technology, Tianjin 300130, China

[c] Prof. W. Zhang
Department of Chemistry, University of Colorado, Boulder, Colorado 80309, United States
E-mail: wei.zhang@colorado.edu (W.Z.)
Supporting information for this article is given *via* a link at the end of the document.

Results and Discussion

To realize the multifunctionality of POCs, benzo[*c*][1,2,5]thiadiazole (BTD) unit with excellent fluorescence property and photocatalytic function has been introduced into a tubular organic cage (MTC1).^[7] The newly prepared MTC1 was characterized by NMR spectroscopy, mass spectrometry, thermogravimetric analysis, single crystal X-ray, and powder X-ray diffraction. As shown in Figures 1a, 1b, and Table S1, MTC1 consists of three BTD units bridged by six cyclohexanediamine segments, forming a tubular structure with the length of 2.1 nm and open triangular windows with side length of ca. 1.6 nm. It is noteworthy that the arrangement of three BTD units in MTC1 shown in Figures 1a and 1b represents the most stable molecular conformation according to the theoretical calculation (Figure S9). Rich heteroatoms, BTD chromophores, and nanometer-sized cavity endow MTC1 the capability of capturing metal ions, detecting metal ions, and even stabilizing ultrafine metal nanoparticles.^[6]

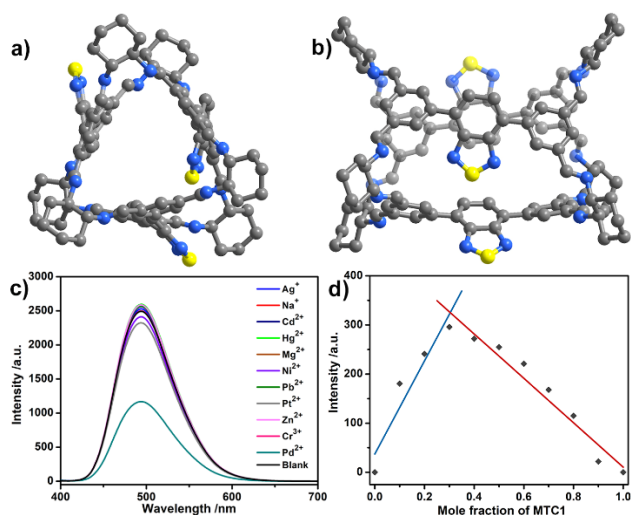


Figure 1. Single crystal structure of MTC1 in top view (a) and side view (b) (C: grey; N: blue; S: yellow; H atoms omitted for clarity); The fluorescence spectra of MTC1 (4.5 $\mu\text{mol L}^{-1}$) in the presence of 10.0 equivalents of different metal ions in DMF (c); Job plot for the binding of MTC1 with Pd²⁺ ions (d).

The electronic absorption spectra of MTC1 in DMF shows the maximum absorption at 380 nm (Figure S10). Upon the excitation at 370 nm (λ_{ex}), the emission spectrum of MTC1 in DMF displays a broad band centred at 494 nm, a relative fluorescence quantum yield $\Phi = 28\%$ with a lifetime of 9.4 ns (Figure S11 and Table S2). Next, the fluorescence response of MTC1 towards different metal ions (including Ag⁺, Na⁺, Cd²⁺, Hg²⁺, Mg²⁺, Ni²⁺, Pb²⁺, Pd²⁺, Pt²⁺, Zn²⁺, and Cr³⁺) was studied. Various metal ions (10 equiv.) were added to a solution of MTC1 in DMF. After 12 hours, the emission of the above solution was measured and compared to the blank, where no metal ions are present except MTC1. As shown in Figure 1c, there was no significant emission change for all other metal ions except Pd²⁺. Only the addition of Pd²⁺ led to serious fluorescence quenching, indicating the selective sensing of MTC1 towards Pd²⁺ likely due

to the chelation-enhanced quenching (CHEQ) effect induced by the interactions between these two species.^[8]

The fluorescence titration curve of MTC1 in DMF discloses that the emission was gradually quenched with increasing amount of Pd²⁺ (Figure S12). According to the titration results, the detection limit of Pd²⁺ was determined to be 38 ppb (based on $3\sigma/k$) (Figure S13). It is worth noting that this detection limit of Pd²⁺ is much lower than the restriction standard 5-10 ppm for the residual palladium metal in body,^[9] demonstrating the outstanding sensing capability of MTC1 towards Pd²⁺. The Pd²⁺ selectivity of this cage sensor was also studied in the presence of various interfering metal ions including Ag⁺, Na⁺, Cd²⁺, Hg²⁺, Mg²⁺, Ni²⁺, Pb²⁺, Pt²⁺, Zn²⁺, and Cr³⁺ (Figure S14). There was a very slight disturbance in the fluorescence quenching of Pd²⁺ in the presence of all metal ions except Pt²⁺. Addition of Pt²⁺ as interfering metal ion led to more significant fluorescence quenching. However, the underlying mechanism of such phenomenon is still unclear at this stage. Two peaks with the binding energies of 336.9 and 342.1 eV corresponding to Pd 3d_{5/2} and Pd 3d_{3/2}, respectively, were observed in the X-ray photoelectron spectrum (XPS) of Pd(II)@MTC1 (Figure S15), confirming the formation of Pd(II)@MTC1 complex. As a consequence of Pd²⁺ complexation with MTC1, the binding energies of 399.3 and 398.4 eV for nitrogen atoms from imine and BTD units, respectively, in MTC1 shift to higher binding energies at 399.6 and 398.6 eV in the N 1s XPS spectrum of Pd(II)@MTC1 (Figure S16), confirming the interactions between Pd²⁺ and imine/BTD nitrogen atoms of MTC1.^[10] In order to gain more insight into the sensing mechanism, a Job plot was obtained, showing a maximum emission intensity at ~0.3 and 1:2 binding stoichiometry between MTC1 and Pd²⁺ (Figure 1d). Even when six equivalents of Pd²⁺ were added to the solution of MTC1, we only observed the complex peaks with 1:1 and 1:2 molar ratio of MTC1 and Pd²⁺ ions in the mass spectrum of the sample (Figure S17), further supporting the preferred binding of only two Pd²⁺ ions inside MTC1. The possible binding sites composed of imine nitrogen atom(s) and one BTD nitrogen atom were suggested to complex with Pd²⁺ as shown in scheme 1. The proposed binding site and the stronger binding of MTC1 with Pd²⁺ ion compared to CC3 (CC3 is an organic cage made up of four 1,3,5-benzaldehyde and six cyclohexanediamine for reference purpose)^[4] were supported by DFT calculations (Figure S18).

As revealed in the sensing section, MTC1 exhibits the effective binding interactions with Pd²⁺. This, in combination with the nanometer-sized cavity of MTC1, might endow MTC1 as a potential ultrafine metal NP support for possible controlled growth of Pd NPs.^{6k} The reduction of Pd²⁺ and MTC1 in the molar ratio of *x* and *y* (*x* and *y* represent the mole number of Pd²⁺ and MTC1, respectively) with excess NaBH₄ was carried out subsequently. A clear color change from yellow to black was observed, indicating the successful reduction of Pd(II) ions into Pd(0) atoms (Figures S19). These cage-based composites are denoted as Pd@MTC1-*x*/*y*. The structure of the cage molecule remains intact with the Pd NPs formed inside the cavity. The ¹H NMR spectrum Pd@MTC1-1/5 is fully consistent with that of the as-synthesized empty cage (Figure S19) The presence of proton

resonance peaks of the imine bonds at 8.30 ppm and the absence of the peaks corresponding to the reduced amine protons confirm the imine groups preserved in the cage even after the formation of Pd NPs. Transmission electron microscopy (TEM) image clearly shows that Pd NPs in Pd@MTC1-1/5 (0.7 wt% of Pd element) are homogeneously dispersed with a narrow size distribution of 1.9 ± 0.4 nm (Figures 2a, 2b, and Table S3). The comparable size of Pd NPs to the MTC1 cavity (~ 2.1 nm) suggests the inclusion of Pd NPs by MTC1. A high-angle annular dark-field scanning transmission electron microscopy (HAADF-STEM) image and energy dispersive X-ray (EDX) mapping analysis of Pd@MTC1-1/5 show the homogeneous distribution of the C, S, N, and Pd elements over the sample (Figures S20 and S21). X-ray photoelectron spectroscopy (XPS) data of Pd@MTC1-1/5 shows two pairs of doublets centred at 335.6 & 340.7 eV and 338.1 & 343.6 eV, which are corresponding to Pd 3d_{5/2} and Pd 3d_{3/2} bands of Pd(0) and Pd(II) species, respectively (Figure 22).^[11] However, in the XPS spectrum of the control sample Pd@CC3-1/5 with Pd NP size of 2.7 ± 0.6 nm, there is only one pair of doublet with binding energies of 335.6 & 340.9 eV corresponding to Pd 3d_{5/2} and Pd 3d_{3/2}, indicating the existence of only zero oxidation state of palladium element (Figure 22). These results suggest that the coordination interaction strength between palladium ions and organic cages might play an important role in controlling the reduction efficiency and the growth/size of NPs under the same reaction conditions. In N 1s XPS spectra, the slightly downshifted binding energies of the nitrogen atoms of the imine groups and BTD units in Pd@MTC1-1/5 were observed in comparison with those in MTC1, supporting the binding interactions between cage and Pd NPs (Figure S23). To further verify Pd NPs anchored inside the MTC1 cavity, ¹H diffusion-ordered spectroscopy (DOSY) NMR spectroscopic measurement was performed on Pd@MTC1-1/5 as well as Pd(II)@MTC1-1/5 and pure MTC1 for comparison purpose (Figures S24-S26 and Table S4). The similar diffusion coefficients for MTC1, Pd(II)@MTC1-1/5, and Pd@MTC1-1/5 with the values of 6.4×10^{-10} , 6.3×10^{-10} , and 6.2×10^{-10} m² s⁻¹, respectively, reveal their similar size and shape, indicating the encapsulation of Pd NPs inside the intra-cage cavity rather than on the cage surface for Pd@MTC1-1/5.^[6a,6b,6i]

With the increase of the molar ratio of Pd²⁺ and MTC1 from 1/5 to 1/2 and 1/1, the size of Pd NPs in Pd@MTC1-1/2 (1.1 wt% Pd) and Pd@MTC1-1/1 (2.0 wt% Pd) increases slightly to 2.1-2.3 nm, which is still comparable with the cage size (Figure S27 and Table S3). Further increasing in the mole ratio of Pd²⁺ and MTC1 not only gradually enlarges the size of Pd NPs in Pd@MTC1-1/0.5 (8.5 wt% Pd), Pd@MTC1-1/0.33 (11.0 wt% Pd), Pd@MTC1-1/0.17 (16.0 wt% Pd), Pd@MTC1-1/0.1 (21.6 wt% Pd), and Pd@MTC1-1/0.033 (28.6 wt% Pd) to 2.7-3.1 nm but also seriously diminishes their solubility.

Palladium NPs have been revealed to exhibit excellent catalytic performance for a couple of organic reactions.^[12] For the purpose of investigating the heterogeneous catalytic activity of a series of cage-supported Pd NPs, the hydride reduction of 4-nitrophenol with NaBH₄ was chosen as a model reaction. In the profile of time-dependent conversion of 4-nitrophenol under

the same conditions, the reaction catalysed by Pd@MTC1-1/5 proceeded most rapidly (Figures 2c, 2d, and Table S3), presumably owing to the smallest particle size thus the highest effective surface area. In addition, the control reactions catalysed by commercially available Pd/C (10 wt% Pd) and Pd@CC3-1/5 with larger particle size proceeded much more slowly, further supporting the notion that excellent catalytic performance of Pd@MTC1-1/5 is likely due to the smaller size of Pd NPs.

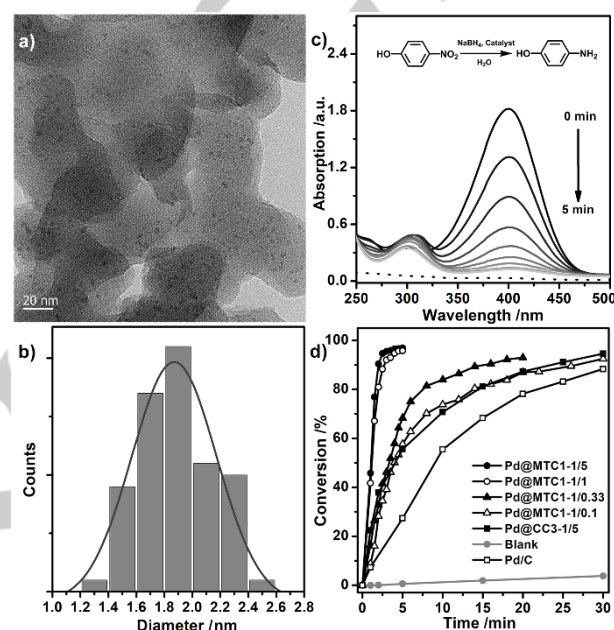


Figure 2. TEM image (a) and Pd nanoparticle size distribution (b) of Pd@MTC1-1/5; Electronic absorption spectra showing the gradual reduction of 4-nitrophenol with NaBH₄ in the presence of heterogeneous Pd@MTC1-1/5 catalyst in H₂O (dashed line: electronic absorption spectrum of Pd@MTC1-1/5 catalyst in H₂O) (c); Time-dependent conversion of 4-nitrophenol with NaBH₄ in the presence of different heterogeneous catalysts (d).

As mentioned above, due to its excellent photocatalytic function, benzo[c][1,2,5]thiadiazole (BTD) unit was introduced to the organic cage MTC1.^[7b] The newly synthesized tubular organic cage is therefore expected to possess good photocatalytic activity. Prior to the investigation of photocatalytic activity, the cyclic voltammetry of MTC1 was measured, which shows its lowest unoccupied molecular orbit (LUMO) energy level of -1.28 V_{SHE} (Figure S28 and Table S2). This energy level is much higher than the reduction potential of -0.33 V_{SHE} for O₂/O₂⁻,^[13,14] suggesting its capability in promoting superoxide radical anion (O₂⁻) evolution under light irradiation via electron transfer process. In the following spin-trapping experiment, the electron spin resonance (ESR) spectroscopy with 5,5-dimethyl-1-pyrroline *N*-oxide (DMPO) as O₂⁻ probe was used to determine the photo-driven product in the presence of solid MTC1. After the irradiation with a blue LED light (420 nm < λ < 490 nm), there appear quartet ESR signals, indicating the evolution of O₂⁻ (Figure S29). This result inspired us to evaluate the photocatalytic performance of MTC1 towards the visible

light-induced aerobic hydroxylation reaction between phenylboronic acid derivatives and $O_2^{\cdot-}$ with *i*Pr₂NEt as sacrificial agent,^[14] (Figure S30).

Table 1. Sequential reactions of photocatalytic aerobic hydroxylation^[a] and hydride reduction of 4-nitrophenylboronic acid (A) to 4-aminophenol (C).

Catalyst	Conv. %		Sel. % ^[b]		Conv. % ^[c]
	A	B ^[d]	D	t/h	
Pd@MTC1-1/5	100	100	0	14.0	95(92) ^[e]
Pd@MTC1-1/1	100	45	55	24.0	— ^[f]
Pd@MTC1-1/0.33	100	28	72	7.0	— ^[f]
Pd@MTC1-1/0.1	100	23	77	7.0	— ^[f]
MTC1	100	100	0	14.0	trace
Pd/C	57	46	54	24.0	— ^[f]

[a] Reaction conditions: 4-nitrophenylboronic acid (60.0 μ mol), catalyst (7.6 mg), *i*Pr₂NEt (300.0 μ mol), CD₃CN (0.8 mL), D₂O (0.2 mL), irradiation with a 25 W blue LED light under a balloon of O₂; [b] The selectivity was deduced on the basis of yield determined by ¹H NMR spectra using 1,4-bis(trimethylsilyl)benzene as an internal standard; [c] reaction conversion in hydride reduction of 4-nitrophenol was determined based on the electronic absorption at 400 nm at short intervals; [d] 4-nitrophenol obtained by visible light-induced aerobic hydroxylation reaction; [e] The reaction conversion shown in the parenthesis is for the reaction catalyzed by Pd@MTC1-1/5, after five successive cycles of visible light-induced aerobic hydroxylation; [f] not available.

Under the irradiation of the same blue LED light in an oxygen atmosphere for 2 hours (14 hours required for 4-nitrophenylboronic acid), a series of phenylboronic acid derivatives substituted with different functional groups are successfully converted into phenol products in the yield of above 99% (Table S5). However, this transformation does not take place in the absence of MTC1 or without irradiation. CC3 is also inactive for this transformation, thus supporting the outstanding photocatalytic performance of MTC1 consisting of BTU units. This, in combination with the good catalytic performance of palladium NPs for hydride reduction as discussed above, renders the possibility of using Pd@MTC1-1/5 as a heterogeneous catalyst to promote the sequential reactions from 4-nitrophenylboronic acid directly to 4-aminophenol in one-pot without separating 4-nitrophenol intermediate. Indeed, under the irradiation of the blue LED light in oxygen atmosphere for 14 hours, Pd@MTC1-1/5 was able to efficiently promote the conversion of 4-nitrophenylboronic acid to 4-nitrophenol in quantitative yield (Table 1). Its catalytic efficiency is just the same as MTC1. Subsequent addition of NaBH₄ into the system led to 95% conversion of 4-nitrophenol (Figure S31). In addition,

it is noteworthy that Pd@MTC1-1/5 can be reused multiple times consecutively in the photo-induced transformation of 4-nitrophenylboronic acid without losing the catalytic activity (Figure S32). It is worth noting that even after five cycles of the catalytic reaction, there was no obvious change in the size of the Pd NPs, compared to the as-synthesized sample, based on the TEM characterization (Figure S34). These results further show the high catalytic activity and stability of Pd@MTC1-1/5. To the best of our knowledge, Pd@MTC1-1/5 represents the first example of the heterogeneous cage-based catalyst to successively catalyze two-step sequential reactions. The catalytic activity of Pd@MTC1-1/1, Pd@MTC1-1/0.33, and Pd@MTC1-1/0.1 in the conversion of 4-nitrophenylboronic acid was also explored. As summarized in Table 1, although we observed quantitative conversion of 4-nitrophenylboronic acid using these catalysts, a significant amount of a side product, 4,4'-dinitro-1,1'-biphenyl (D) was formed. The selectivity of 4-nitrophenol formation was decreased from 100% for Pd@MTC1-1/5 to 45, 28, and 23% for Pd@MTC1-1/1, Pd@MTC1-1/0.33, and Pd@MTC1-1/0.1, respectively. These results suggest that the larger Pd NPs with their size exceeding the cage host in Pd@MTC1-1/1, Pd@MTC1-1/0.33, and Pd@MTC1-1/0.1 promotes photo-induced bimolecular coupling of 4-nitrophenylboronic acid to form the side product D. In contrast, in Pd@MTC1-1/5, the Pd NPs reside inside the cage host and do not affect the visible light-induced aerobic hydroxylation of 4-nitrophenylboronic acid, yet still significantly facilitate the hydride reduction of 4-nitrophenol to 4-aminophenol, indicating the critical role of cage confinement in the present sequential reactions. At the end of this section, it should be mentioned that incomplete conversion reactions over Pd@MTC1-1/1, Pd@MTC1-1/0.33, and Pd@MTC1-1/0.1 preclude further investigation over their catalytic performance in the subsequent hydride reduction step within sequential reactions.

Conclusion

In summary, a highly fluorescent and photocatalytically active organic cage has been synthesized, which exhibits effective and selective binding towards palladium ions. This in turn leads to the development of a cage-supported catalyst containing highly dispersed ultrafine palladium nanoparticles with a narrow size distribution. The excellent photocatalytic activity of this organic cage, in cooperation with the prominent catalytic ability of the ultrafine nanoparticles inside the cage, enable the high-yielding catalytic sequential visible light-induced aerobic hydroxylation and subsequent hydride reduction reactions. This represents the first example of the heterogeneous cage-based catalyst that can be operated in water. We also revealed the size effect of Pd NPs and synergistic effect between Pd NPs and organic cage during the sequential catalysis. The knowledge gained in this study would open new possibilities for developing functional organic cages targeting diverse applications in different fields.

Acknowledgements

Financial support from the Natural Science Foundation of China (Nos. 21631003 and 21805005), the Fundamental Research Funds for the Central Universities (No. FRF-BD-17-016A), University of Science and Technology Beijing, University of Colorado Boulder, and K. C. Wong Education Foundation is gratefully acknowledged.

Keywords: porous organic cage • palladium • ultrafine nanoparticles • photocatalysis • sequential catalysis

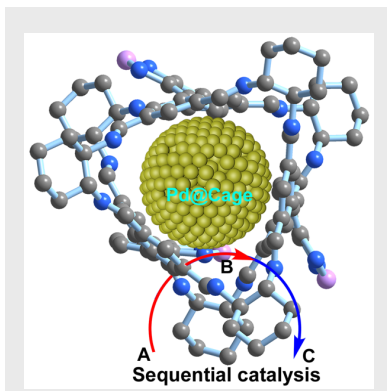
- [1] a) H. Furukawa, K. E. Cordova, M. O'Keeffe, O. M. Yaghi, *Science* **2013**, *341*, 1230444; b) J. D. Xiao, H. L. Jiang, *Acc. Chem. Res.* **2019**, *52*, 356-366; c) Y. Bai, Y. Dou, L. H. Xie, W. Rutledge, J. R. Li, H. C. Zhou, *Chem. Soc. Rev.* **2016**, *45*, 2327-2367; d) B. Li, H. M. Wen, Y. Cui, W. Zhou, G. Qian, B. Chen, *Adv. Mater.* **2016**, *28*, 8819-8860; e) T. Drake, P. F. Ji, W. B. Lin, *Acc. Chem. Res.* **2018**, *51*, 2129-2138; f) N. C. Burch, H. Jasuja, K. S. Walton, *Chem. Rev.* **2014**, *114*, 10575-10612; g) J. R. Li, J. L. Sculley, H. C. Zhou, *Chem. Rev.* **2012**, *112*, 869-932; h) W. L. He, M. Zhao, C. D. Wu, *Angew. Chem. Int. Ed.* **2019**, *58*, 168-172; i) A. Schoedel, M. Li, D. Li, M. O'Keeffe, O. M. Yaghi, *Chem. Rev.* **2016**, *116*, 12466-12535; j) L. Li, R. B. Lin, R. Krishna, H. Li, S. Xiang, H. Wu, J. Li, W. Zhou, B. Chen, *Science* **2018**, *362*, 443-446; k) M. Zhao, K. Yuan, Y. Wang, G. Li, J. Guo, L. Gu, W. Hu, H. Zhao, Z. Tang, *Nature* **2016**, *539*, 76-80; l) Q. Xia, Z. Li, C. Tan, Y. Liu, W. Gong, Y. Cui, *J. Am. Chem. Soc.* **2017**, *139*, 8259-8266.
- [2] a) S. Lin, C. S. Diercks, Y. B. Zhang, N. Kornienko, E. M. Nichols, Y. Zhao, A. R. Paris, D. Kim, P. Yang, O. M. Yaghi, C. J. Chang, *Science* **2015**, *349*, 1208-1213; b) A. G. Slater, A. I. Cooper, *Science* **2015**, *348*, aaa8075; c) X. Y. Guan, H. Li, Y. C. Ma, M. Xue, Q. R. Fang, Y. S. Yan, V. Valtchev, S. L. Qiu, *Nat. Chem.* **2019**, *11*, 587-594; d) X. Feng, X. S. Ding, D. L. Jiang, *Chem. Soc. Rev.* **2012**, *41*, 6010-6022; e) X. Han, J. Huang, C. Yuan, Y. Liu, Y. Cui, *J. Am. Chem. Soc.* **2018**, *140*, 892-895; f) K. Wang, D. Qi, Y. Li, T. Wang, H. Liu, J. Jiang, *Coord. Chem. Rev.* **2019**, *378*, 188-206.
- [3] a) R. M. Barrer, V. H. Shanson, *J. Chem. Soc., Chem. Commun.* **1976**, *9*, 333-334; b) M. Simard, D. Su, J. D. Wuest, *J. Am. Chem. Soc.* **1991**, *113*, 4696-4698; c) N. B. McKeown, *J. Mater. Chem.* **2010**, *20*, 10588-10597; d) T. Adachi, M. D. Ward, *Acc. Chem. Res.* **2016**, *49*, 2669-2679; e) R. B. Lin, Y. B. He, P. Li, H. L. Wang, W. Zhou, B. Chen, *Chem. Soc. Rev.* **2019**, *48*, 1362-1389; f) I. Hisaki, C. Xin, K. Takahashi, T. Nakamura, *Angew. Chem. Int. Ed.* **2019**, *58*, 2-13; g) B. Han, H. Wang, C. Wang, H. Wu, W. Zhou, B. Chen, J. Jiang, *J. Am. Chem. Soc.* **2019**, *141*, 8737-8740. h) I. Sinha, P. S. Mukherjee, *Inorg. Chem.* **2018**, *57*, 4205-4221 and reference therein; i) P. Das, A. Kumar, P. Howlader, P. S. Mukherjee, *Chem. Eur. J.* **2017**, *23*, 12565-12574; j) R. Chakrabarty, P. S. Mukherjee, P. J. Stang, *Chem. Rev.* **2011**, *111*, 6810-6918; k) D. C. Caskey, T. Yamamoto, C. Addicott, R. K. Shoemaker, J. Vacek, A. M. Hawkrige, D. C. Muddiman, G. S. Kottas, J. Michl, P. J. Stang, *J. Am. Chem. Soc.* **2008**, *130*, 7620-7628; l) J. Vacek, D. C. Caskey, D. Horinek, R. K. Shoemaker, P. J. Stang, J. Michl, *J. Am. Chem. Soc.* **2008**, *130*, 7629-7638.
- [4] a) S. Durot, J. Taesch, V. Heitz, *Chem. Rev.* **2014**, *114*, 8542-8578; b) X. S. Ke, T. Kim, Q. He, V. M. Lynch, D. Kim, J. L. Sessler, *J. Am. Chem. Soc.* **2018**, *140*, 16455-16459; c) T. Hasell, A. I. Cooper, *Nat. Rev. Mater.* **2016**, *1*, 16053; d) M. Mastalerz, *Acc. Chem. Res.* **2018**, *51*, 2411-2422; e) R. D. Mukhopadhyay, Y. Kim, J. Koo, K. Kim, *Acc. Chem. Res.* **2018**, *51*, 2730-2738; f) T. P. Money Penny, N. P. Walter, Z. Cai, Y. R. Miao, D. L. Gray, J. J. Hinman, S. Lee, Y. Zhang, J. S. Moore, *J. Am. Chem. Soc.* **2017**, *139*, 3259-3264; g) M. Mastalerz, M. W. Schneider, I. M. O'Connell, O. Presly, *Angew. Chem. Int. Ed.* **2011**, *50*, 1046-1051; h) J. T. A. Jones, T. Hasell, X. Wu, J. Bacsa, K. E. Jelfs, M. Schmidtman, S. Y. Chong, D. J. Adams, A. Trewin, F. Schiffman, F. Cora, B. Slater, A. Steiner, G. M. Day, A. I. Cooper, *Nature* **2011**, *474*, 367-371; i) C. Zhang, Z. Wang, L. Tan, T. L. Zhai, S. Wang, B. Tan, Y. S. Zheng, X. L. Yang, H. B. Xu, *Angew. Chem. Int. Ed.* **2015**, *54*, 9244-9248; j) L. Chen, P. S. Reiss, S. Y. Chong, D. Holden, K. E. Jelfs, T. Hasell, M. A. Little, A. Kewley, M. E. Briggs, A. Stephenson, K. M. Thomas, J. A. Armstrong, J. Bell, J. Busto, R. Noel, J. Liu, D. M. Strachan, P. K. Thallapally, A. I. Cooper, *Nat. Mater.* **2014**, *13*, 954-960; k) K. Acharyya, P. S. Mukherjee, *Angew. Chem. Int. Ed.* **2019**, *58*, 8640-8653; l) T. Tozawa, J. T. A. Jones, S. I. Swamy, S. Jiang, D. J. Adams, S. Shakespeare, R. Clowes, D. Bradshaw, T. Hasell, S. Y. Chong, C. Tang, S. Thompson, J. Parker, A. Trewin, J. Bacsa, A. M. Z. Slawin, A. Steiner, A. I. Cooper, *Nat. Mater.* **2009**, *8*, 973-978; m) Y. H. Jin, Q. Wang, P. Taynton, W. Zhang, *Acc. Chem. Res.* **2014**, *47*, 1575-1586; n) L. Zhang, L. Xiang, C. Hang, W. Liu, W. Huang, Y. Pan, *Angew. Chem. Int. Ed.* **2017**, *56*, 7787-7791; o) P. T. Smith, B. P. Benke, Z. Cao, Y. Kim, E. M. Nichols, K. Kim, C. J. Chang, *Angew. Chem. Int. Ed.* **2018**, *57*, 9684-9688; p) Q. Q. Wang, N. Luo, X. D. Wang, Y. F. Ao, Y. F. Chen, J. M. Liu, C. Y. Su, D. X. Wang, M. X. Wang, *J. Am. Chem. Soc.* **2017**, *139*, 635-638; q) C. Zhang, Z. Wang, L. Tan, T. L. Zhai, S. Wang, B. Tan, Y. S. Zheng, X. L. Yang, H. B. Xu, *Angew. Chem. Int. Ed.* **2015**, *54*, 9244-9248; r) H. Qu, Y. Wang, Z. Li, X. Wang, H. Fang, Z. Tian, X. Cao, *J. Am. Chem. Soc.* **2017**, *139*, 18142-18145; s) H. Ding, Y. Yang, B. Li, F. Pan, G. Zhu, M. Zeller, D. Yuan, C. Wang, *Chem. Commun.* **2015**, *51*, 1976-1979; t) G. Yu, T.-Y. Cen, Z. He, S.-P. Wang, Z. Wang, X.-W. Ying, S. Li, O. Jacobson, S. Wang, L. Wang, L.-S. Lin, R. Tian, Z. Zhou, Q. Ni, X. Li, X. Chen, *Angew. Chem. Int. Ed.* **2019**, *58*, 8799-8803.
- [5] a) C. X. Zhang, Q. Wang, H. Long, W. Zhang, *J. Am. Chem. Soc.* **2011**, *133*, 20995-21001; b) J. X. Song, N. Aratani, H. Shinokubo, A. Osuka, *J. Am. Chem. Soc.* **2010**, *132*, 16356-16357; c) Y. Shi, K. Cai, H. Xiao, Z. Liu, J. Zhou, D. Shen, Y. Qiu, Q. H. Guo, C. Stern, M. R. Wasielewski, F. Diederich, W. A. Goddard, J. F. Stoddart, *J. Am. Chem. Soc.* **2018**, *140*, 13835-13842; d) Y. H. Jin, C. Yu, R. J. Denman, W. Zhang, *Chem. Soc. Rev.* **2013**, *42*, 6634-6654; e) Z. Wang, N. Sikdar, S. Q. Wang, X. Li, M. Yu, X. H. Bu, Z. Chang, X. Zou, Y. Chen, P. Cheng, K. Yu, M. J. Zaworotko, Z. Zhang, *J. Am. Chem. Soc.* **2019**, *141*, 9408-9414; f) J. Jiao, C. Tan, Z. Li, Y. Liu, X. Han, Y. Cui, *J. Am. Chem. Soc.* **2018**, *140*, 2251-2259.
- [6] a) B. Mondal, P. S. Mukherjee, *J. Am. Chem. Soc.* **2018**, *140*, 12592-12601; b) R. McCaffrey, H. Long, Y. Jin, A. Sanders, W. Park, W. Zhang, *J. Am. Chem. Soc.* **2014**, *136*, 1782-1785; c) M. Nihei, H. Ida, T. Nibe, A. M. P. Moeljadi, Q. T. Trinh, H. Hirao, M. Ishizaki, M. Kurihara, T. Shiga, H. Oshio, *J. Am. Chem. Soc.* **2018**, *140*, 17753-17759; d) G. J. Chen, W. L. Xin, J. S. Wang, J. Y. Cheng, Y. B. Dong, *Chem. Commun.* **2019**, *55*, 3586-3589; e) X. Yang, J. K. Sun, M. Kitta, H. Pang, Q. Xu, *Nat. Catal.* **2018**, *1*, 214-220; f) Y. Zhang, Y. Xiong, J. Ge, R. Lin, C. Chen, Q. Peng, D. Wang, Y. Li, *Chem. Commun.* **2018**, *54*, 2796-2799; g) J. K. Sun, W. Zhang, T. Akita, Q. Xu, *J. Am. Chem. Soc.* **2015**, *137*, 7063-7066; h) S. Y. Zhang, Z. Kochovski, H. C. Lee, Y. Lu, H. Zhang, J. Zhang, J. K. Sun, J. Y. Yuan, *Chem. Sci.* **2019**, *10*, 1450-1456; i) L. Qiu, R. McCaffrey, Y. H. Jin, Y. Gong, Y. M. Hu, H. L. Sun, W. Park, W. Zhang, *Chem. Sci.* **2018**, *9*, 676-680; j) L. Qiu, R. McCaffrey, W. Zhang, *Chem. Asian J.* **2018**, *13*, 362-372; k) B. Mondal, K. Acharyya, P. Howlader, P. S. Mukherjee, *J. Am. Chem. Soc.* **2016**, *138*, 1709-1716.
- [7] a) A. Mallick, A. M. El-Zohry, O. Shekha, J. Yin, J. T. Jia, H. Aggarwal, A. Emwas, O. F. Mohammed, M. Eddaoudi, *J. Am. Chem. Soc.* **2019**, *141*, 7245-7249; b) K. Zhang, D. Kopetzki, P. H. Seeberger, M. Antonietti, F. Vilela, *Angew. Chem. Int. Ed.* **2013**, *52*, 1432-1436.
- [8] a) G. Aragay, J. Pons, A. Merkoç, *Chem. Rev.* **2011**, *111*, 3433-3458; b) J. M. Da, browski, B. Pucelik, A. Regiel-Futyr, M. Brindell, O. Mazuryk, A. Kyzioł, G. Stochel, W. Macyk, L. G. Arnaut, *Coord. Chem. Rev.* **2016**, *325*, 67-101.
- [9] a) B. Liu, Y. Y. Bao, F. F. Du, H. Wang, J. Tian, R. K. Bai, *Chem. Commun.* **2011**, *47*, 1731-1733; b) D. H. Dai, Z. Li, J. Yang, C. Y. Wang, J. R. Wu, Y. Wang, D. M. Zhang, Y. W. Yang, *J. Am. Chem. Soc.* **2019**, *141*, 4756-4763.

- [10] a) S. Y. Ding, J. Gao, Q. Wang, Y. Zhang, W. G. Song, C. Y. Su, W. Wang, *J. Am. Chem. Soc.* **2011**, *133*, 19816-19822; b) Y. Q. Chen, Z. Wang, Y. W. Wu, S. R. Wisniewski, J. X. Qiao, W. R. Ewing, M. D. Eastgate, J. Q. Yu, *J. Am. Chem. Soc.* **2018**, *140*, 17884-17894.
- [11] a) M. Trzeciak, A. W. Augustyniak, *Coord. Chem. Rev.* **2019**, *384*, 1-20; b) S. Lu, Y. Hu, S. Wan, R. McCaffrey, Y. Jin, H. Gu, W. Zhang, *J. Am. Chem. Soc.* **2017**, *139*, 17082-17088.
- [12] a) Q. H. Yang, Q. Xu, S. H. Yu, H. L. Jiang, *Angew. Chem. Int. Ed.* **2016**, *55*, 3685-3689; b) A. Biffi, P. Centomo, A. D. Zotto, M. Zecca, *Chem. Rev.* **2018**, *118*, 2249-2295; c) F. Raza, D. Yim, J. H. Park, H. I. Kim, S. J. Jeon, J. H. Kim, *J. Am. Chem. Soc.* **2017**, *139*, 14767-14774; d) D. Astruc, F. Lu, J. R. Aranzaes, *Angew. Chem. Int. Ed.* **2005**, *44*, 7852-7872; e) Y. B. Huang, Q. Wang, J. Liang, X. S. Wang, R. Cao, *J. Am. Chem. Soc.* **2016**, *138*, 10104-10107.
- [13] L. Ma, Y. Liu, Y. Liu, S. Jiang, P. Li, Y. Hao, P. Shao, A. Yin, X. Feng, B. Wang, *Angew. Chem. Int. Ed.* **2019**, *58*, 4221-4226.
- [14] P. F. Wei, M. Z. Qi, Z. P. Wang, S. Y. Ding, W. Yu, Q. Liu, L. K. Wang, H. Z. Wang, W. K. An, W. Wang, *J. Am. Chem. Soc.* **2018**, *140*, 4623-4631.

Entry for the Table of Contents

RESEARCH ARTICLE

Excellent photocatalytic activity of porous organic cage, in cooperation with cage-supported ultrafine palladium nanoparticles, enables the sequential reactions including visible light-induced aerobic hydroxylation and hydrogenation



Nana Sun, Chiming Wang, Hailong Wang,* Le Yang, Peng Jin, Wei Zhang,* Jianzhuang Jiang*

Page 1 – Page 5

Multifunctional Tubular Organic Cage-Supported Ultrafine Palladium Nanoparticles for Sequential Catalysis

Accepted Manuscript